

## A statistical method for determining intrinsic electronic transport properties of self-assembled alkanethiol monolayer devices

Hyunwook Song and Takhee Lee<sup>a)</sup>

Department of Materials Science and Engineering, Gwangju Institute of Science and Technology, Gwangju 500-712, Korea

Nak-Jin Choi and Hyoyoung Lee

National Creative Research Initiative, Center for Smart Molecular Memory, Electronics and Telecommunications Research Institute, Daejeon 305-350, Korea

(Received 19 October 2007; accepted 1 December 2007; published online 20 December 2007)

We present a statistical method to investigate the electronic transport of molecular devices. Electrical characterizations are performed with subsequent statistical analysis on 6745 molecular devices with nanometer-scale junction diameter. The comprehensive temperature-variable current-voltage measurements are also performed to elucidate the dominant charge conduction mechanism responsible for intrinsic molecular transport properties. The entity of data acquired represents a reliable basis for statistical analysis, which consequently provides an objective criterion to determine the most probable transport characteristics of molecular devices. © 2007 American Institute of Physics. [DOI: 10.1063/1.2827239]

The nature of electronic transport through the organic molecules sandwiched between metallic electrodes is of primary significance in building reliable molecular devices.<sup>1</sup> To date, even if some insights into the transport mechanism have been demonstrated by employing a variety of different molecules and experimental techniques,<sup>1</sup> large disparities in the experimental data (on even nominally identical samples) have prevented a clear understanding of electronic transport in the molecular systems.<sup>2</sup> Since the transport characteristics in metal-molecule junctions are subject to stochastic fluctuation,<sup>3,4</sup> statistical analysis and interpretation of data are necessary for an objective criterion to obtain the intrinsic characteristics of molecular devices.

Here, we present a statistical method to investigate the electronic transport of molecular devices. For this, comprehensive temperature-variable current-voltage [ $I(V, T)$ ] characterization has been performed with subsequent statistical analysis, using mass-fabricated molecular devices with nanometer-scale junction diameter. The  $I(V, T)$  characterization can play a critical role in determining the transport mechanism which makes it possible, for example, to distinguish electronic tunneling transport from thermally activated conduction such as impurity-mediated transport.<sup>5</sup> A study based on the statistical approach would give impartiality in determining the intrinsic molecular transport properties.

In this study, we used alkanethiol [ $\text{CH}_3(\text{CH}_2)_{n-1}\text{SH}$ ] self-assembled monolayers (SAMs), one of the molecular systems that have been extensively studied.<sup>3,5-7</sup> Figure 1(a) shows the device structure, where alkanethiol SAMs are sandwiched between two metallic contacts through a nanowell.<sup>8</sup> The junction diameter is estimated to be  $\sim 50$  nm from a cross-sectional scanning electron microscope (SEM) image of the nanowell [Fig. 1(b)].

We examined a total of 6745 molecular devices fabricated employing the alkanethiol SAMs of various chain lengths at room temperature. Of these devices examined, we found 6244 devices (92.6%) with linear  $I(V)$  and current in

the milliampere range. This indicates a metallic short caused by the penetration of the vapor-deposited top electrode through the molecular layer. Also, we found 19 devices (0.3%) with no detectable current in the subpicoampere range, which is likely due to a failure during the device fabrication such as an incomplete etching of the  $\text{Si}_3\text{N}_4$  insulating layer. In addition, 482 devices (7.1%) showed nonlinear  $I(V)$  characteristics and current in the nanoampere range, which corresponds to the general characteristics of metal-molecule-metal junctions under investigation. To investigate electronic transport properties from this last group of candidate molecular devices, we performed temperature-variable current-voltage [ $I(V, T)$ ] characterization, through which we identified the transports in four different categories: (i) direct tunneling, (ii) Fowler-Nordheim tunneling, (iii) thermally activated conduction, and (iv) Coulomb blockade phenomenon.

Figures 2(a)–2(g) show the characteristic behaviors of different transports over  $\pm 1$  V range observed from four representative devices. In direct tunneling, no significant temperature dependence of the transport characteristics is observed [Figs. 2(a) and 2(b)]. Based on the applied bias as compared to barrier height ( $\Phi_B$ ), the tunneling transports can be divided into either direct ( $V < \Phi_B/e$ ) or Fowler-Nordheim ( $V > \Phi_B/e$ ) tunneling. These two tunneling mechanisms can be distinguished by their distinct current-voltage dependencies.<sup>9</sup> The molecular devices in direct tunneling do not exhibit an inflection point on a plot of  $\ln(I/V^2)$  vs  $1/V$  as shown in Fig. 2(b). This is consistent with tunneling through

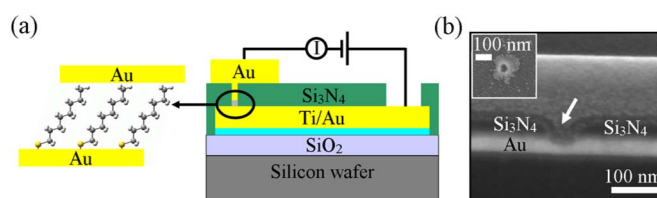


FIG. 1. (Color online) (a) Schematic of the molecular device structure. (b) A SEM image of a nanowell (marked by the arrow) in cross-sectional view. The inset shows a nanowell in top view. The scale bars are 100 nm.

<sup>a)</sup>Electronic mail: tlee@gist.ac.kr.

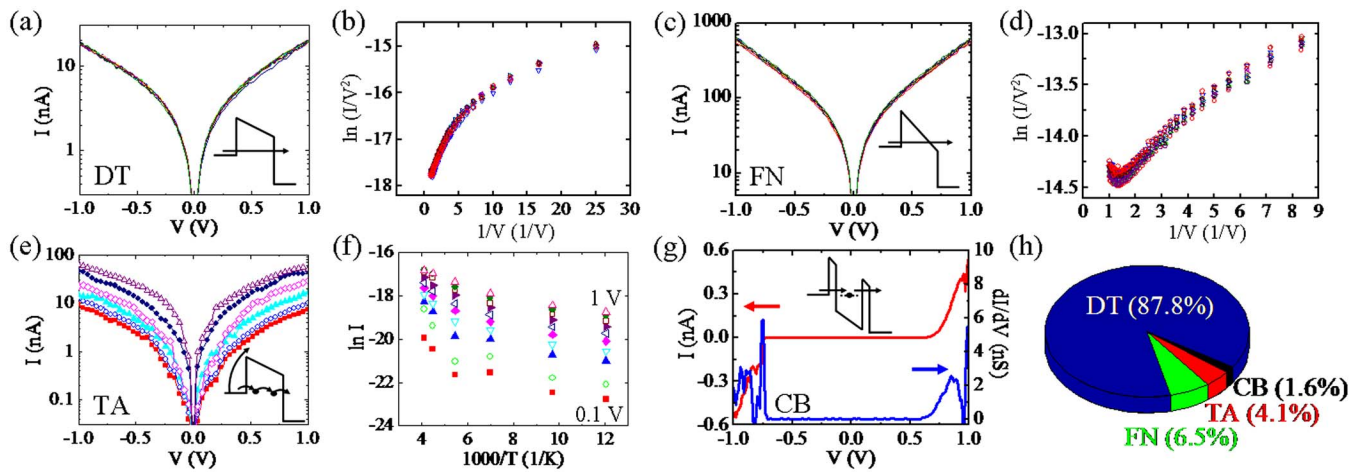


FIG. 2. (Color online) (a)–(g) show the characteristic behaviors of various transports observed from four representative devices. (a)  $I(V, T)$  data of a direct tunneling (DT) device in 300–80 K. (b) Plots of  $\ln(I/V^2)$  vs  $1/V$  of (a). (c)  $I(V, T)$  data of a Fowler-Nordheim (FN) tunneling device in 300–80 K. (d) Plots of  $\ln(I/V^2)$  vs  $1/V$  of (c). (e)  $I(V, T)$  data of a thermal-activated (TA) conduction device in 300–80 K. (f) Arrhenius plots ( $\ln I$  vs  $1/T$ ) of (e). (g)  $I(V)$  data (red line) of a Coulomb blockade (CB) device at 80 K and corresponding numerical differential conductance ( $dI/dV$ ) (blue line). (h) A pie chart summarizing the statistics of various transports observed in this study.

a trapezoidal barrier when the applied bias is less than the barrier height. Fowler-Nordheim tunneling also shows no temperature-dependent characteristics [Figs. 2(c) and 2(d)], which is analogous to direct tunneling. However, at a high-voltage regime when the applied bias exceeds the barrier height, the barrier shape is changed from trapezoidal to triangular barrier, and the conduction mechanism causes a transition on a plot of  $\ln(I/V^2)$  vs  $1/V$ . This gives rise to a linear decay region at the high-bias tail as shown in Fig. 2(d).<sup>10</sup> Figures 2(e) and 2(f) show the charge transport in which thermal activation is involved. It has an obvious temperature-dependent  $I(V)$  behavior, which can be identified by an Arrhenius plot ( $\ln I$  vs  $1/T$ ) [Fig. 2(f)]. For such devices, the conduction mechanism shows a large device-to-device fluctuation with activation energy in hundreds of meV depending on a specific temperature and voltage range, which thereby further complicates the analysis. These temperature-dependent  $I(V)$  characteristics may result from impurity-mediated transport components.<sup>5,11</sup> Occasionally, as in Fig. 2(g), the current is strongly suppressed near the zero voltage, whereas the current abruptly increases at high voltages, and the corresponding numerical differential conductance shows large conductance gap. This can be due to the Coulomb blockade effect. In these samples, it is likely that the Au atoms which were separated from the vapor-deposited top electrode migrated into the SAM, forming a localized state in molecular junctions.<sup>12</sup> This results in forming a double-barrier tunnel junction incorporating a Au nanoparticle in the SAM. The width of the zero conductance region can be approximately determined by  $e/C$  ( $C$  is the capacitance).<sup>13</sup> The capacitance formed between the Au particle and the electrode can be estimated from the normalized capacitance  $C/4\pi\epsilon r$  with respect to the dependence of the normalized position ( $z/r$ ) in a mirror image point-charge model of a charged sphere (radius  $r$ ) at the distance  $z$  from the electrode.<sup>14</sup> By considering the relative permittivity of alkanethiol as 2.6,<sup>15</sup> the molecular length, and the position of Au particle ( $z$ ) from the electrode, it is roughly estimated that the Au particle radius ( $r$ ) is less than  $\sim 0.3$  nm. The estimated particle radius corresponds to the size of the Coulomb

island formed in the junction and is enough small to be incorporated into the alkanethiol SAMs.

Figure 2(h) summarizes the percentage of statistical distribution for which we observe each of the various transports based on the comprehensive  $I(V, T)$  characterizations. We obtained a total of 123  $I(V, T)$  data in a complete temperature range of 300–80 K.<sup>16</sup> Among them, 108 devices (87.8%) showed direct tunneling characteristics in accordance with temperature-independent  $I(V)$  characteristics and no transition on a plot of  $\ln(I/V^2)$  vs  $1/V$ . Thus, as the most probable occurrence, the statistical assessment demonstrates that direct tunneling is indeed the dominant charge transport mechanism in the alkanethiol molecular devices. The dominance of direct tunneling in alkanethiol SAMs is in good agreement with previous reports<sup>5,7</sup> and can be reasonably anticipated due to their large highest occupied molecular orbital–lowest unoccupied molecular orbital gap ( $\sim 8$  eV). However, as shown in Fig. 2(h), an uncontrolled device-to-device variation in transport mechanisms indicates the importance of a statistical study.

Repeated measurements give a statistical picture of molecular transport properties, typically presented as histograms. Figure 3 shows histograms for the conductance measured at the Ohmic region inside  $\pm 0.1$  V. The data of devices governed by all different transport mechanisms (Fig. 2) exhibit the linear  $I(V)$  characteristics inside  $\pm 0.1$  V and this linear portion of individual  $I(V)$  curve is used to estimate a junction conductance from the slope. For creating the histograms, we take all the  $I(V)$  curves measured without any data selection or processing. Thereby, the histograms faithfully exhibit the intact device statistics. In Fig. 3, blue-filled columns represent the conductance histograms for all the fabricated 6745 devices measured at room temperature and red-patterned columns represent those for 108 direct tunneling devices confirmed from the acquired 123  $I(V, T)$  data as explained above. The histograms exhibit the appearance of an intermediate regime excluding typical nonworking devices such as short or open junctions. The appearance of such an intermediate regime in the histograms is unambiguously different in the absence of molecules. As an example, the his-

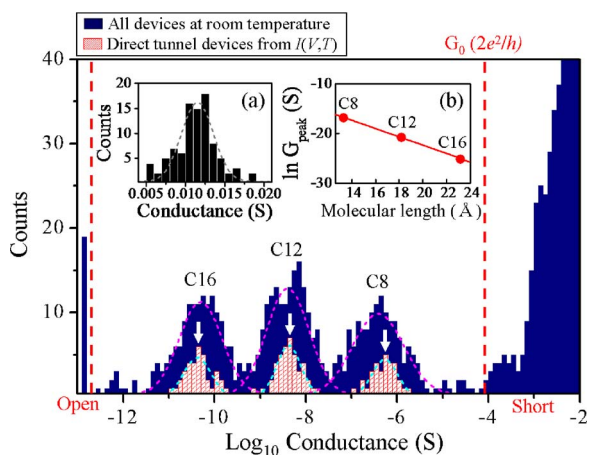


FIG. 3. (Color online) Conductance histograms for all devices (blue-filled columns) measured at room temperature and the direct tunneling devices (red-patterned columns) confirmed by  $I(V,T)$  characterizations. The Gaussian curves (dashed lines) highlight the conductance peaks for each alkanethiol. Inset (a) is a conductance histogram for the intentional short devices in the absence of molecules. Inset (b) shows a logarithmic plot of conductance peak values (marked by the arrows) vs molecular length.

togram for short devices intentionally made without molecules is plotted in inset (a) of Fig. 3. Therefore, we ascribe this intermediate regime to the formation of a molecular junction in which, depending on the molecular length of alkanethiols (marked as C16, C12, and C8), the conductance values vary over orders of magnitude and appear to be distributed log normally with well-defined conductance peaks highlighted by the Gaussian curves for each alkanethiol. Note that the log-normal distribution of the conductance values stems from a parameter that affects the conductance exponentially and is therefore likely due to a variation in tunneling distance.<sup>17,18</sup> This effect is not observed in the absence of molecules where the devices show linearly normal distribution in the histogram [see inset (a) in Fig. 3].<sup>19</sup> The variation in tunneling distance could be attributed to detailed microscopic configurations of metal-molecule junctions in numerous degrees of freedom such as contact distance, molecular binding site, surface structure of electrodes, and molecular conformations and orientations.<sup>4,20</sup>

The peak positions in the conductance histograms of three different length alkanethiols for the direct tunneling devices (red-patterned columns) are identified by the arrows in Fig. 3, representing the most probable measured conductance value for the molecular device.<sup>3</sup> To determine the decay coefficient ( $\beta$ ) for the direct tunneling devices,<sup>3,7</sup> the conductance values are plotted as a function of molecular length, as shown in inset (b) of Fig. 3. The conductance value exponentially depends on the molecular length, according to  $G \sim \exp(-\beta d_m)$  ( $G$  is the conductance and  $d_m$  is the molecular length). Our data can be described by the above relationship, with  $\beta = 0.86 \pm 0.02 \text{ \AA}^{-1}$ , which is consistent with previous reports.<sup>3,7</sup>

In conclusion, we reported a statistical method to study the intrinsic electronic transport of molecular devices (using

6745 fabricated and measured alkanethiol devices). The comprehensive temperature-variable current-voltage characterization for candidate molecular devices monitors the full categories of transport properties. Our statistical analysis shows that direct tunneling is indeed the dominant conduction mechanism responsible for the intrinsic transport properties of alkanethiol molecular devices. The conductance histograms are well consistent with the tunneling characteristics and show log-normal distribution in conductance values, which is the result of a variation in tunneling distance. The statistical method can introduce an objective criterion for the examination of intrinsic electronic transport of molecular devices.

We thank Y. Majima for the helpful discussions on the Coulomb blockade phenomenon. This work was supported by the National Research Laboratory (NRL) Program and the Basic Research Program of the Korea Science and Engineering Foundation, and the Program for Integrated Molecular System at GIST. H.L. acknowledges the support of Creative Research Initiatives (Smart Molecular Memory) of MOST/KOSEF, Korea.

- <sup>1</sup>N. J. Tao, *Nat. Nanotechnol.* **1**, 173 (2006), and references therein.
- <sup>2</sup>S. M. Lindsay and M. A. Ratner, *Adv. Mater. (Weinheim, Ger.)* **19**, 23 (2007).
- <sup>3</sup>S.-Y. Jang, P. Reddy, A. Majumdar, and R. A. Segalman, *Nano Lett.* **6**, 2362 (2006).
- <sup>4</sup>E. Lörtscher, H. B. Weber, and H. Riel, *Phys. Rev. Lett.* **98**, 176807 (2007).
- <sup>5</sup>W. Wang, T. Lee, and M. A. Reed, *Rep. Prog. Phys.* **68**, 523 (2005).
- <sup>6</sup>H. Song, H. Lee, and T. Lee, *J. Am. Chem. Soc.* **129**, 3806 (2007).
- <sup>7</sup>W. Wang, T. Lee, and M. A. Reed, *Phys. Rev. B* **68**, 035416 (2003).
- <sup>8</sup>See EPAPS Document No. E-APPLAB-91-074752 for the experimental details associated with the device fabrication and electrical characterization. This document can be reached through a direct link in the online article's HTML reference section or via the EPAPS homepage (<http://www.aip.org/pubservs/epaps.html>).
- <sup>9</sup>S. M. Sze, *Physics of Semiconductor Devices*, 2nd ed. (Wiley, New York, 1981).
- <sup>10</sup>J. M. Beebe, B. Kim, J. W. Gadzuk, C. D. Frisbie, and J. G. Kushmerick, *Phys. Rev. Lett.* **97**, 026801 (2006).
- <sup>11</sup>E. E. Polymeropoulos and J. Sagiv, *J. Chem. Phys.* **69**, 1836 (1978).
- <sup>12</sup>L. H. Yu, C. D. Zangmeister, and J. G. Kushmerick, *Phys. Rev. Lett.* **98**, 206803 (2007).
- <sup>13</sup>A. E. Hanna and M. Tinkham, *Phys. Rev. B* **44**, 5919 (1991).
- <sup>14</sup>Y. Azuma, M. Kanehara, T. Teranishi, and Y. Majima, *Phys. Rev. Lett.* **96**, 016108 (2006).
- <sup>15</sup>M. A. Rampi, O. J. A. Schueller, and G. M. Whitesides, *Appl. Phys. Lett.* **72**, 1781 (1998).
- <sup>16</sup>A number of devices failed during the  $I(V,T)$  characterization likely due to continuous electric and thermal sweeps. For reliability, we only considered the devices where the conduction mechanism is confirmed by the repeated  $I(V)$  measurements in a sufficient wide temperature range (300–80 K).
- <sup>17</sup>V. B. Engelkes, J. M. Beebe, and C. D. Frisbie, *J. Phys. Chem. B* **109**, 16801 (2005).
- <sup>18</sup>T. W. Kim, G. Wang, H. Lee, and T. Lee, *Nanotechnology* **18**, 315204 (2007).
- <sup>19</sup>The distribution of conductance values would result from a variation of junction geometry such as contact area, as the conductance depends linearly on contact area according to Ohm's law.
- <sup>20</sup>Y. Hu, Y. Zhu, H. Gao, and H. Guo, *Phys. Rev. Lett.* **95**, 156803 (2005).